

Design and fabrication of an indigenous confined bubble column: Investigation of single bubble ascent

Sikandar Almani ^{a,*}, Muhammad Raheel Bawani ^b, Ubedullah Ansari ^c, Masroor Abro ^a, Mashad Akhund ^a, Ali Abbas ^a

^a *Process Simulation and Modeling Research Group, Department of Chemical Engineering, Mehran University of Engineering and Technology, Jamshoro, Pakistan*

^b *Department of Mining Engineering, Mehran University of Engineering and Technology, Jamshoro, Pakistan*

^c *Institute of Petroleum and Natural Gas Engineering, Mehran University of Engineering and Technology, Jamshoro, Pakistan*

* Corresponding author: Sikandar Almani, Email: sikander.almani@faculty.muet.edu.pk

Received: 06 January 2025, Accepted: 27 March 2025, Published: 01 April 2025

KEYWORDS

Gas-liquid interaction
Confined bubble column
Shadowgraphy
Single bubble
Terminal velocity

ABSTRACT

In Chemical Process Industries (CPIs) like petrochemicals, biochemicals, and pharmaceuticals, gas-liquid interactions are crucial. Bubble columns are preferred for their low maintenance, absence of moving parts, and efficient mass transfer and mixing. Liquid phases in such systems often shift from Newtonian to non-Newtonian behavior, as seen in materials like molasses, cooking oil, and microalgae, affecting hydrodynamic parameters like gas holdup, mixing time and mass transfer. This study investigated single-bubble dynamics using an Indigenous confined bubble column ($6 \times 240 \times 1140 \text{ mm}^3$) in water (Newtonian) and CarboxyMethyl Cellulose (CMC) solutions (non-Newtonian) at 1 g/L, 2 g/L, and 3 g/L. The shadowgraphy technique measured bubble size, terminal velocity, Reynolds number, bubble count, and trajectory. In water, bubbles measured 1.48 mm, with sizes increasing to 1.87 mm and 2.08 mm in 2 g/L and 3 g/L CMC due to higher viscosity delaying detachment. Terminal velocity was 0.22 m/s in water, dropping to 0.11 m/s, 0.107 m/s, and 0.088 m/s in 1 g/L, 2 g/L, and 3 g/L CMC, respectively. Reynolds numbers declined sharply from 335.2 in water to 31.5, 7.9, and 3.5 in CMC solutions, reflecting viscosity's inverse effect. Bubble count increased from 7 per frame in water to 14, 15, and 17 in CMC solutions, as lower terminal velocity prolonged bubble presence. Trajectories were zigzag in water but remained rectilinear in CMC solutions across all concentrations. These findings highlight rheology's significant impact on bubble behavior, which will be essential for optimising process parameters in various CPIs.

1. Introduction

Gas-liquid interaction refers to the behavior of gas and liquid when they come into contact with each other. This interaction is fundamental to many chemical and industrial processes, including chemical reactions, separation, mass transfer, and mixing. When a liquid is exposed to a gas, it can create bubbles, which rise to the surface of the liquid. The bubbles provide a large interfacial area between the gas and the liquid,

allowing for efficient mass transfer and mixing of reactants. The size and shape of the bubbles and the rate at which they rise depend on factors such as gas flow rate, liquid properties, and reactor design [1-3,10,11-16]. In summary, in a variety of chemical and industrial processes, the interaction between gas and liquid is crucial, and optimizing the gas-liquid interface is essential to achieve efficient and effective transfer of mass and energy. For gas-liquid interaction,

various devices have been employed for industrial purposes and laboratory research such as tray columns, packed columns and Bubble columns.

A bubble column is a type of reactor used in chemical engineering for gas-liquid reactions, mixing, and mass transfer. The column typically consists of a tall liquid-filled vertical tube, in which gas is introduced at the bottom of the column through a gas sparger, which can be designed in different configurations, including single or multiple gas spargers, flat or concave bottoms, and different sizes and aspect ratios [5, 17-23]. As gas is introduced into the liquid, it rises to the surface in the form of bubbles, creating turbulence and helping to mix the liquid. The bubbles provide a large interfacial area between the gas and the liquid, allowing for efficient mass transfer and mixing of reactants. Bubble columns have a number of advantages, including low energy consumption, high gas holdup, easy scale-up, and minimal maintenance requirements. They are employed in numerous industrial settings, including fermentation [24], Microalgae culture [3], and wastewater treatment [25]. However, a bubble column's effectiveness and efficiency may be impacted by variables including bubble size, gas flow rate, liquid characteristics, and reaction kinetics. The careful creation and use of bubble columns are required to achieve optimal performance and ensure safety.

As discussed earlier, the rheological behavior of the liquid phase changes from Newtonian to non-Newtonian especially for microalgae culture [26]. That's why to ensure the proper light distribution in the photobioreactor (PBR), it is necessary to reduce the specific illuminated area which is only possible by reducing the thickness of the PBR. Keeping in view, the thin gap bubble column [27, 4, 6] and thin film technologies [28] were developed.

In the present study, the confined bubble column is used, which consists of a tall vertical rectangular column with a small gap (6 mm) between the walls. In a confined bubble column, gas is introduced at the bottom of the column, and bubbles rise up through the liquid in the gap between the tube walls [2, 4, 6]. The small size of the column also minimizes the liquid holdup and pressure drop, making it a cost-effective and energy-efficient reactor. Confined bubble columns are used in a variety of industrial and research applications, including fermentation, biochemistry, and wastewater treatment. Besides the thin configuration, the rheological change of the liquid phase during operations in CPIs also makes the hydrodynamics complex inside gas-liquid contactors. For describing the rheological characteristics of non-

Newtonian fluids in a variety of applications, such as food processing, cosmetics, and polymer manufacturing, the power-law model is frequently utilized. It provides a simple and effective means to characterize the behavior of these materials under different shear conditions. A recent study has been investigated using high-speed imaging in a bubble column Reactor. A recent study has been conducted using high-speed imaging in a bubble column Reactor. In this study, single bubble ascent in Newtonian (water) and non-Newtonian (CMC and XG) liquid phases was investigated in a newly fabricated indigenous confined bubble column. The effect of continuous phase rheology/viscosity on bubble shape, terminal velocity, Reynolds number, Number of bubbles and trajectory were studied.

2. Material and Methods

2.1 Experimental Setup

The confined bubble column was fabricated with two vertical sheets of 12 mm thickness and a frame of 6 mm between them joined together with the nuts and bolts. It is made up of transparent PolyAcrylic Acid (PAA) PAA acrylic material to facilitate the visualization / Shadowgraphy experimental studies (where the gas phase is investigated between the optical lamp and camera)[2, 4]. The working size of this bubble column is about (6 x 240 x 1140 mm³) and has 1 capillary of $d_{cap} = 0.75$ mm at the bottom of the column, which is designed to release single gas bubbles into the liquid, the capillary is joined with an air compressor by a 1 mm pipe as shown in Fig. 1. The column is securely mounted and sealed to prevent leakages.

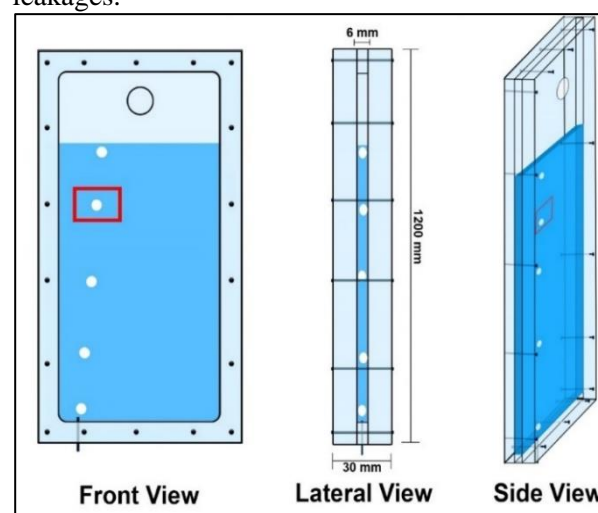


Fig. 1. Schematic diagram of Confined Bubble Column

For Shadowgraphy, a Digital Single-Lens Reflex (DSLR) D-400 was used to monitor and record the behavior of bubbles in the column. A high-resolution camera and LED lamp were fixed in the same optical axis to capture images of the bubbles as they ascend

from the column's base as shown in Fig. 2. The camera has a resolution of 1500 x 1100 pixels and is equipped with a fixed focal lens of 60 mm, with a variable aperture from 2.5 to 30 and a maximum frequency of 12 Hz, to capture the size of bubble, terminal velocity, number of bubbles and trajectory of the rising bubbles. The LED lamp provides sufficient illumination for the camera to capture clear images of the bubbles. The shadowgraphy measurement zone ($10 \times 10 \text{ cm}^2$) is located at a height of 800 mm from the bottom of the column. This position, corresponding to the above mid-height of the column, was chosen to make sure that bubbles have reached their terminal velocity. The capillary is positioned 5 cm from the lateral wall. This distance is considered sufficient to avoid wall influence on the hydrodynamics of isolated bubbles [29]. Air bubbles are generated using a low-pressure air compressor joined with the Flow Meter having a range of about 0-250 mL/h.

2.2 Shadowgraphy Experiments and Measurement Methods

Shadowgraphy measurements can be a powerful tool for studying fluid flow in a confined bubble column. In this type of column, the gap between the gas sparger and the column wall is very narrow, which can make it difficult to study the flow patterns using other measurement techniques.

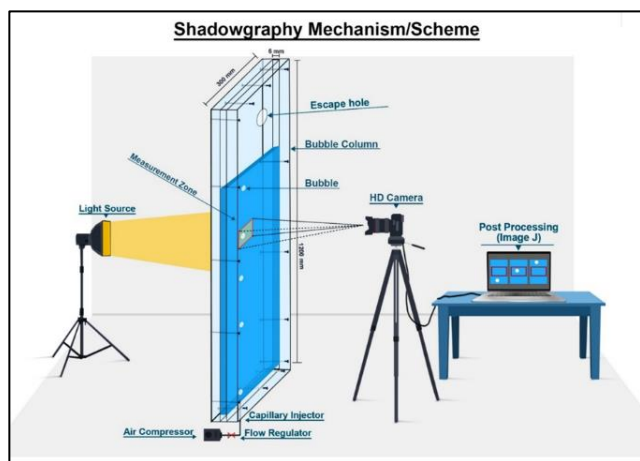


Fig. 2. Schematic Diagram of Bubble Column Experimental Setup

To perform shadowgraphy measurements in a confined bubble column, an illumination/ light source is used to illuminate the fluid in the column (Fig. 3). The light passes through the fluid and is refracted by the density variations caused by the bubbles rising through the liquid. This creates a shadow pattern on a screen or camera, which can be used to study the bubble's behavior.

A shadowgraphy method is used to gauge the bubble size, terminal velocity, number of bubbles in the frame and bubble trajectory which information can

be further used to optimize the performance of the Confined Bubble Column for various applications. The fluid under study is positioned between the light source and the camera, which are aligned along the same optical axis, in this optical flow visualization technique. Using a synchronization system, the camera records images at the lighting system's predetermined pulsation frequency. The camera has a resolution of 1500 x 1100 pixels and is equipped with a fixed focal lens of 60 mm, with a variable aperture from 2.5 to 30 and a maximum frequency of 12 Hz. The imaging frequency is always captured at its highest level. Since bubbles are always in the same plane in our confined column case, this kind of measurement is possible. This method works well for bubbles where light rays travelling through the bubble's edge deflate it, creating a shadow area. Therefore, the equivalent diameter " d_b " is the diameter of a sphere with a projected area equal to that of the measured bubble [4].



Fig. 3. Bubble column Exp Setup

2.2.1 Bubble equivalent diameter (d_b) determination

To calculate bubble equivalent diameter in ImageJ, preprocess the image (grayscale, enhance contrast, threshold) and isolate bubbles. Use Analyze > Analyze Particles and enable "Equivalent Diameter" in Set Measurements. The results table will display the diameter of each bubble derived from its area.

2.2.2 Terminal velocity (V_t) measurements

By dividing the horizontal and vertical displacements of the gravity centre between two frames by the

interval between two captured images, one may calculate the horizontal and vertical components of the bubble velocity. The terminal velocity is then calculated using only the vertical component of the velocity of the single bubble rising in the column. we can then calculate the Bubble's terminal velocity (V_t) can be calculated employing the following formula:

$$V_t = \frac{S}{t} \quad (\text{Eq. 1})$$

where,

V_t = terminal velocity of the bubble in (m/sec).

S = distance (in meters) the bubble travelled between two images

t = time interval between two images (in seconds).

2.2.3 Non-Newtonian Reynolds number (R_e) measurements

The Reynolds Number of a single bubble rising in a 6 mm gap bubble column with different fluids is also calculated by using the formula proposed by Almani et al.[2].

$$R_{econf} = \frac{\rho_L \times d_b (e - d_b)^{n-1} V_t^{2-n}}{K^{2n-1}} \quad (\text{Eq. 2})$$

Where:

R_{econf} = Reynolds number for confined geometry.

ρ_L = the fluid density.

d_b = the bubble diameter.

V_t = the terminal velocity of bubble.

e = Gap Width.

n = the Power Law index

K = the Consistency index

2.2.4 Bubble trajectory measurements

The captured images are analyzed using image processing techniques (Image J Software) to obtain information about the bubble trajectory using trajectory protocol. where all images in the measurement zone are arranged to maintain the same frame of reference. To analyze a bubble's trajectory in ImageJ, load the image stack, preprocess (enhance contrast, threshold, and filter), and use TrackMate tool for tracking. Export the x, y coordinates for analysis and plot the trajectory. Visualize the results by overlaying the trajectory on the images and saving the output.

2.2.5 Number of bubbles count (nb) measurements

Image J Software was also used to detect and count bubbles in shadowgraphy images and can be used for

thresholding and particle analysis tools to identify and quantify bubbles. To count bubbles in ImageJ, load the image, convert it to grayscale, enhance contrast, and apply thresholding to isolated bubbles. Use Analyze > Analyze Particles with appropriate size/shape filters to detect and count bubbles. Results, including the total count, will be displayed and summarized.

2.3 Fluid and its Physicochemical and Rheological Properties

The rheological behavior of the operating fluid changes from Newtonian to non-Newtonian fluids during the operations in Chemical Process Industries (CPI). Therefore, we have selected three Aqueous solutions of CMC (1 g/L, 2 g/L and 3 g/L) as a non-Newtonian model fluid to mimic the high-concentration conditions. Whereas water is used as a reference fluid. Physicochemical and Rheological Properties are shown in Table 1. In this table, the values of K and n of CMC Solutions are taken from [30].

Table 1

Physico-chemical and rheological Properties of fluids.

Parameter	Fluid			
	Tap water	CMC (1 g/L)	CMC (2 g/L)	CMC (3 g/L)
ρ (kg/m ³)	1000	1001.2	1001.3	1001.6
σ (N/m)	0.0728	0.0692	0.0674	0.0661
K (Pa.s)	0.001	0.008	0.082	0.189
n (-)	1	0.9	0.7	0.63
T (°C)	22	22	22	22

The power-law model for non-Newtonian fluids can be expressed mathematically using the following equation to model the viscosity of non-Newtonian Fluids:

$$\tau = K \cdot \dot{\gamma}^{n-1} \quad (\text{Eq. 3})$$

Where τ is the shear stress, K is the consistency coefficient, $\dot{\gamma}$ is the shear rate, and n is the flow behavior index. The flow behavior index determines the extent to which the fluid exhibits shear-thinning or shear-thickening behavior. A value of n less than 1 indicates shear-thinning behavior, while a value of n greater than 1 indicates shear-thickening behavior. When n equals 1, the fluid exhibits Newtonian behavior.

3. Results and Discussion

The findings of the current experimental work on the fabricated 6 mm confined bubble column are presented here. We verified the accuracy of our results by comparing them with previously published research papers [31, 32]. Shadowgraphy method was

used to calculate the bubble sizes, terminal velocity, Reynolds number, Number of bubbles and trajectory in the bubble column. Water is utilized as the reference liquid and CMC with concentrations (1 g/L, 2 g/L and 3 g/L) are used as mimic fluids depicting the high concentrations in industry process fluids. In this study, ImageJ software is used to determine bubble size, number of bubbles and bubble trajectories. In the context of our study in the 6 mm gap bubble column, the determination of terminal velocity played a significant role in understanding the behavior of rising bubbles within this specific column.

3.1 Effect of Rheology on the Bubble Diameter

The effect of liquid phase rheology on the bubble diameter was observed in this confined column where in the reference case of water, the bubble size was estimated at around 1.48 mm which is the lowest in comparison to all other CMC solutions (Fig. 4). This can be explained as water has a relatively lower viscosity than other non-Newtonian solutions, resulting in relatively easier generation of small bubbles with minimal resistance. The bubble size in CMC concentration of 1 g/L remained consistent with water, which is equal to 1.48 mm. whereas, for other solutions of CMC 2 g/L and 3 g/L the bubble size enlarges to 1.86 mm and 2.08 mm respectively (Table 2).

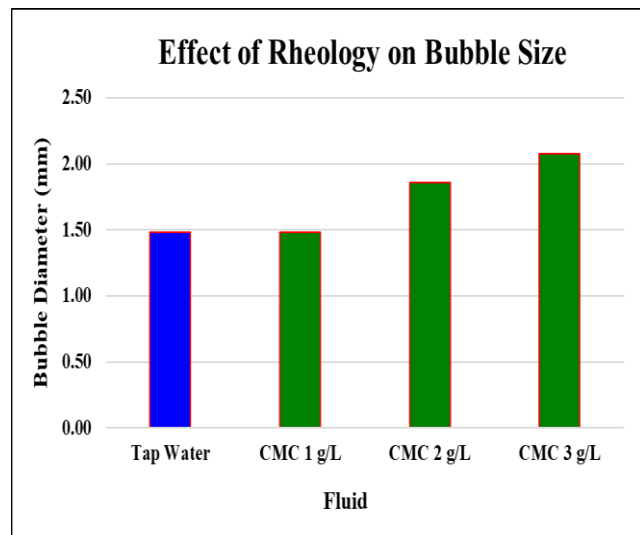


Fig 4. Effect of Rheology on Bubble Size

Table 2

Bubble Characteristics in various fluids

Fluid	Bubble Diameter (mm)	Terminal Velocity (m/s)	Reynolds Number (-)
Tap water	1.48	0.226	335.27
CMC (1 g/L)	1.48	0.115	31.52
CMC (2 g/L)	1.86	0.107	7.89
CMC (3 g/L)	2.08	0.088	3.95

This is mainly due to the viscous effect where bubble detachment takes time in high-viscosity fluid hence increasing bubble volume which corroborates in increasing the bubble diameter [33]. The results obtained from the current experiments illustrate that the rheological effect on bubble size is most pronounced with higher CMC concentrations. The increased viscosity of CMC solutions hinders bubble coalescence, resulting in larger bubble diameters. The choice of liquid phase and its rheological properties plays a crucial role in determining bubble size.

3.2 Effect of Rheology on the Terminal Velocity

The experimental terminal velocities are evaluated inside an indigenous bubble column of width 240 mm height of 1140 mm and 6 mm thickness. The experimental results presented in this study are derived from a thorough analysis of bubble terminal velocity in water and three aqueous CMC solutions. For $d_b = 1.48$ mm rising in water, the terminal velocity was calculated 0.226 m/s. whereas for the CMC solutions of 1 g/L, 2 g/L and 3 g/L the values of V_t are 0.114 m/s, 0.106 m/s and 0.088 m/s respectively (Fig. 5). CMC significantly increases the viscosity of the liquid, leading to a notable reduction in terminal velocity. Fig. 5 shows that bubbles encounter greater resistance while rising through the viscous CMC solution compared to water.

The change in rheology leads to a substantial increase in viscosity compared to water. The elevated viscosity introduces greater resistance to the rising bubbles, causing a notable decrease in terminal velocity Fig. 5 and 6 consequently, bubbles will ascend more slowly in CMC solutions [2, 34]. The impact on liquid density is likely to be minor, and therefore, any changes in buoyancy and terminal velocity due to density are expected to be limited.

To provide context for our findings, we conducted a comparative analysis with previously reported experimental data and correlations, specifically referencing the work of Clift et al. [31] as shown in (Fig. 6), the results of Clift et al. [31] are of bubbles rising in an infinite column, where there is no effect of the wall. This comparative approach enhances our understanding of the dynamics and behavior of bubbles within our experimental system. We conducted a comparative analysis between our research findings and the results reported by [32] as shown Fig. 6, which collectively confirm that an increase in viscosity, as induced by CMC addition, consistently leads to a decrease in bubble's terminal velocity.

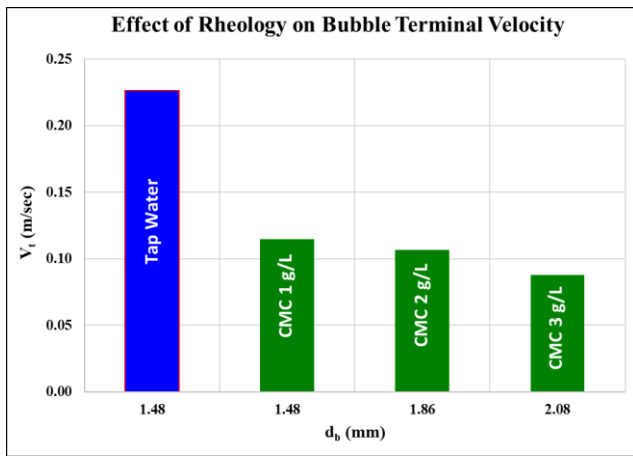


Fig. 5. Effect Of Rheology On Bubble Terminal Velocity

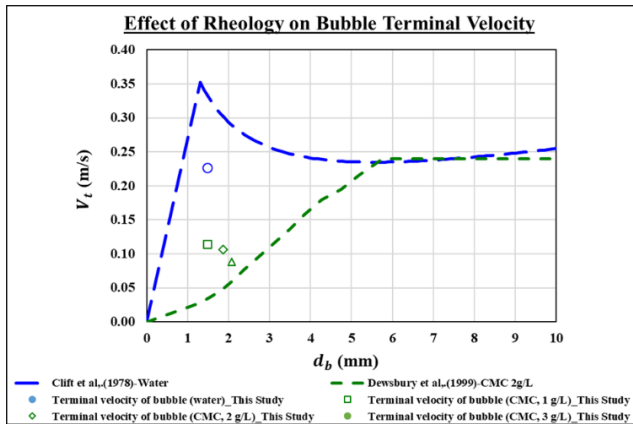


Fig. 6. Overall Effect Of Rheology On Bubble Terminal Velocity Of Water, CMC At Concentrations of 1 g/L, 2 g/L, and 3 g/L As The Liquid Phase Compared To (Dewsbury et al., 1999), (Clift et al, 1978).

The overall effect of rheology on bubble terminal velocity in this bubble column, considering water as a reference and CMC at concentrations of 1 g/L, 2 g/L, and 3 g/L as the liquid phase, can be succinctly summarized. In this study, the influence of rheological properties, primarily viscosity, is prominently demonstrated. Water, with its lower viscosity, allows bubbles to ascend relatively unhindered, resulting in higher terminal velocities. However, as CMC concentration increases, so does the solution's viscosity, and this heightened viscosity presents substantial resistance to bubble motion. Consequently, bubbles experience progressively slower ascent in CMC solutions.

3.3 Reynolds Number

The Reynolds number (Re) is a dimensionless number used to predict the flow regime in a fluid system. To determine whether the flow is laminar or turbulent in confined geometry, the Reynolds number (Re) can be calculated using the following formula developed by Almani et al. [2] for the bubble rising in a confined environment.

The Reynolds number was calculated for water and CMC solutions using the physicochemical properties

provided in Table 1. Bubbles with a diameter of 1.48 mm in water attain a terminal velocity of 0.226 m/s, resulting in a relatively high Reynolds number of 335.27 as shown Fig. 7. This high Reynolds number is indicative of a turbulent flow regime, which is attributed to the low viscosity and high terminal velocity of bubbles in water. Bubbles of the same size (1.48 mm) in a CMC solution at a concentration of 1 g/L exhibit a significantly lower terminal velocity (0.115 m/s) and a reduced Reynolds number to 31.52. These reduced values suggest a flow regime that is less turbulent, and in fact, they may even indicate a laminar flow regime due to the increased viscosity of the CMC solution.

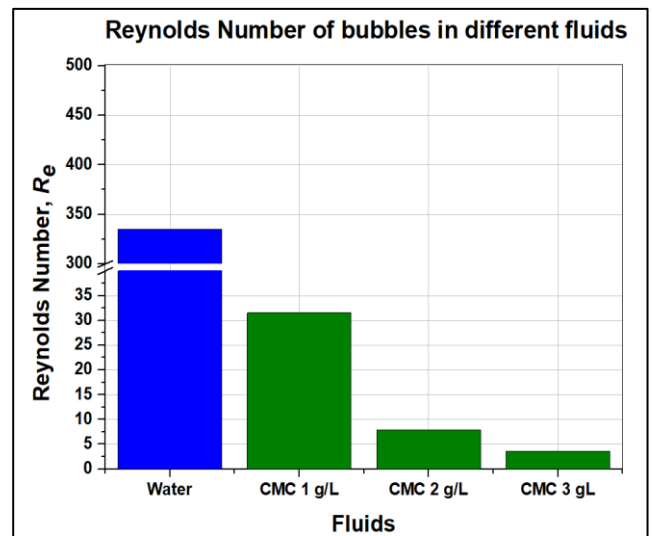


Fig. 7. Relationship Between Reynolds Number (Re) And Bubble Diameter

When the CMC concentration increases to 2 g/L, accompanied by a slightly larger bubble diameter (1.86 mm), the terminal velocity further decreases to 0.107 m/s. The Reynolds number, which is calculated at 7.89, is lower compared to the 1g/L CMC solution. Finally, in the CMC solution with the highest concentration of 3 g/L and larger bubbles (2.08 mm), the terminal velocity decreases to 0.088 m/s. Notably, the Reynolds number, calculated as 3.59, is significantly lower compared to CMC solutions at 1 g/L and 2 g/L as shown in Fig. 7. In this study the specific relationship between bubble diameter and Reynolds number is observed and can be highly complex and depends on factors like bubble size distribution, bubble rise velocity, and the fluid's properties.

In our research, we have observed a noteworthy relationship between the bubble diameter, viscosity, and the Reynolds number (Re) within a CMC solution. As the bubble diameter increases in this solution, there is a discernible decrease in the Reynolds number. This phenomenon is in alignment with fundamental principles of fluid mechanics. Moreover, when the

viscosity of the CMC solution increases, it also leads to a reduction in the Reynolds number. This observation is further supported by previous studies in the field, such as the work of Almani et al. [2], which also found that an increase in both bubble size and viscosity results in lower Reynolds numbers, particularly within CMC solutions. The consistent trend across these studies underscores the substantial impact of rheological properties on the behavior of bubbles within fluid systems. In practical terms, this relationship between bubble size, viscosity, and Reynolds number has significant implications for flow dynamics within the CMC solution. Smaller bubbles and lower Reynolds numbers are associated with more orderly and less turbulent flow patterns. In contrast, larger bubbles and higher Reynolds numbers tend to promote increased turbulence and mixing, affecting the overall flow behavior. This intricate interplay between rheological properties and bubble behavior sheds light on the complex dynamics of fluid systems and offers valuable insights into various applications, particularly within CMC solutions.

3.4 Number of Bubbles

This research investigates the impact of rheological properties on bubble formation within various liquid mediums. We examined the influence of liquid viscosity and density on the quantity of bubbles produced. Our experiments were conducted with both pure water and CMC solutions at different concentrations. The findings revealed a consistent trend – as the liquid's viscosity increased, the number of bubbles also increased (Fig. 8). This phenomenon highlights the intriguing relationship between rheology and bubble behavior and has implications for a broader understanding of fluid dynamics in diverse applications.

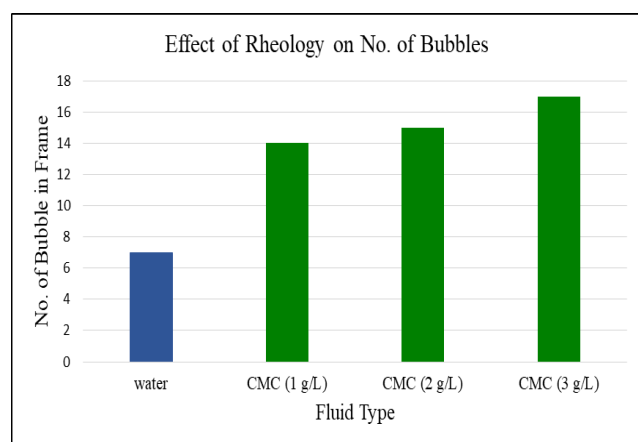


Fig. 8. Effect of Rheology on Number of Bubbles (d_b)

In the context of pure water, we explored the direct effect of rheology on the number of bubbles. Our observations indicated that changes in rheological properties, such as viscosity and density, led to

variations in the number of bubbles formed within the defined 10 x 10 cm² square reference frame/zone. In water, an average of 7 bubbles were observed in a frame as shown in Fig. 8. Shifting our focus to CMC solutions with a concentration of 1 g/L, we continued to investigate the impact of rheology on bubble formation. In this case, a noticeable increase in the number of bubbles was observed, with an average of 14 bubbles within the observation frame. In the study of CMC solutions with a concentration of 2 g/L, our observations revealed an increase in the number of bubbles, with an average of 15 bubbles within the observation frame. Extending our exploration to CMC solutions with a concentration of 3 g/L, our findings showed a significant rise in the number of bubbles. The average number of bubbles within the observation frame was 17 as shown in Fig. 8. This section provides insight into the impact of even higher CMC concentrations on bubble dynamics and the role of rheology in this context. To explain this phenomenon, it can be stated that increasing viscosity will decrease the terminal velocity of the bubble hence more bubbles appear in observation frame in the same time frame compared to water which is why we have a higher number of bubbles in CMC solutions.

3.5 Bubble Trajectory

The effect of rheology on bubble trajectory in a bubble column is a critical aspect of understanding how fluid properties shape the behavior of bubbles within the system. Rheology, primarily influenced by fluid viscosity, has a substantial impact on the trajectory of bubbles. When the liquid in the column exhibits higher viscosity, bubbles encounter increased resistance as they ascend. This heightened resistance can result in deviations from a straightforward, vertical trajectory. Bubbles may follow more meandering or turbulent paths due to their enhanced interaction with the viscous liquid. But in the confined bubble column, in CMC solutions, bubbles have rectilinear trajectories due to confined configuration and high viscosity. Whereas in water, the trajectory is zigzag/non-rectilinear mainly due to low viscosity. In this study for bubble trajectory in a bubble column with water as the liquid phase and bubble diameter measuring 1.48 mm as shown in Fig. 9a, in water, bubbles typically exhibit a relatively straightforward and nearly vertical trajectory with small bubble oscillations during their ascent in a 6 mm gap. The low viscosity of water results in minimal resistance to bubble motion, allowing them to rise with minimal deviation from the vertical path. The bubble trajectory in the bubble column with CMC 1 g/L as the liquid phase and 1.48 mm bubble diameter as shown in Fig. 9b. The combination of increased fluid viscosity due to CMC

and the specific bubble size influences bubble trajectory. Bubbles of this size encounter resistance as they rise through the viscous CMC solution, resulting in deviations from a strictly vertical trajectory. In this experiment, we tracked and analyzed the trajectory of 14 bubbles using ImageJ software as shown in Fig. 9b. Furthermore, for the higher viscosity introduced by the CMC solution at 2 g/L, combined with the larger bubble diameter, results in pronounced effects on bubble motion. Bubbles of this size encounter substantial resistance as they rise through the viscous CMC solution, leading to deviations from a strictly vertical trajectory. In this experiment, we tracked the trajectory of 15 bubbles using ImageJ software as shown in Fig. 9c. Similarly for 3 g/L as the liquid phase and 2.08 mm bubble diameter as shown in Fig. 9d. The CMC solution's elevated viscosity due to the higher concentration and the larger bubble diameter combined to significantly influence bubble motion. Bubbles of this size experience substantial resistance as they ascend through the viscous CMC solution, leading to deviations from a purely vertical trajectory.

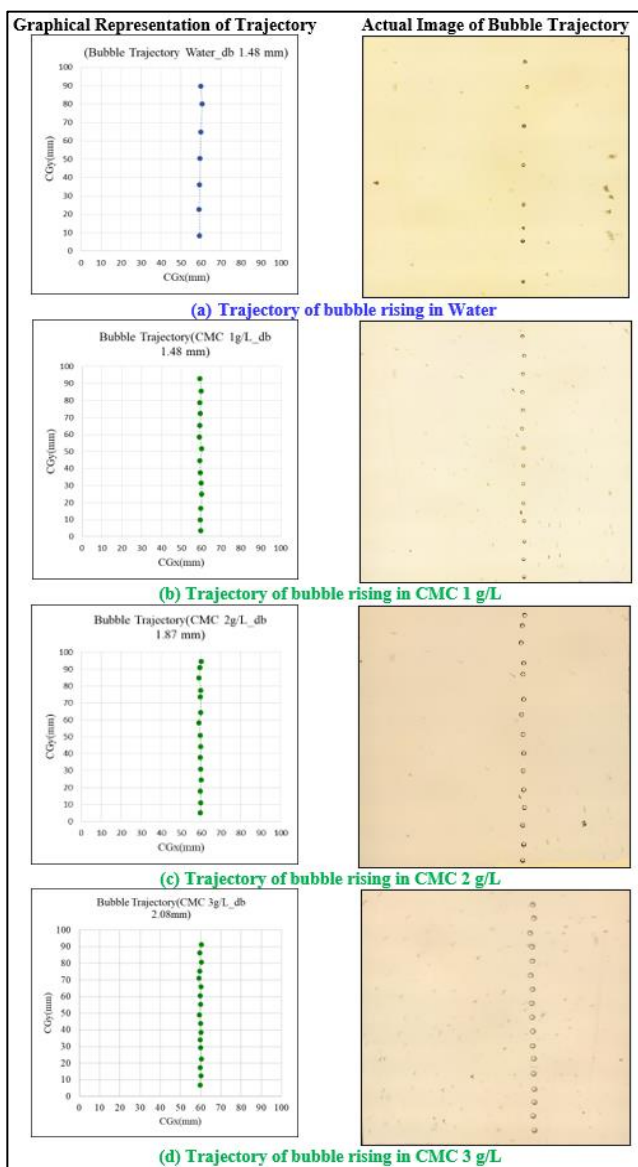


Fig. 9. Bubble Trajectory In Fluids

In this study, we observe the overall effect of rheology on bubble trajectory in a bubble column with water, CMC at different concentrations (1 g/L, 2 g/L, and 3 g/L), and varying bubble diameters (ranging from 1.48 mm to 2.08 mm) as the liquid phase reveals a distinct correlation between viscosity and bubble trajectory (Fig. 10). In water, where viscosity is low, bubbles with a 1.48 mm diameter follow a nearly vertical trajectory having 7 bubbles in trajectory Frame with few oscillations. As CMC concentration and bubble size increase, there is a noticeable shift in behavior. In CMC 1 g/L, where viscosity is slightly high, bubbles with a 1.48 mm diameter follow a nearly vertical trajectory having 14 bubbles in trajectory Frame which is clearly greater than water. In CMC 2 g/L, where viscosity is higher compared with water and CMC 1 g/L, bubbles with a 1.87 mm diameter follow a very nearly vertical trajectory having 15 bubbles in trajectory Frame which is also clearly greater than water and CMC 1 g/L solution. In CMC 3 g/L, where viscosity is higher as compared with water, CMC 1 g/L and CMC 2 g/L, bubbles with a 2.08 mm diameter follow a very nearly vertical trajectory as compared with water and other low concentrated solution having 17 bubbles in trajectory Frame which is also clearly greater than water and other low Concentrated CMC solutions.

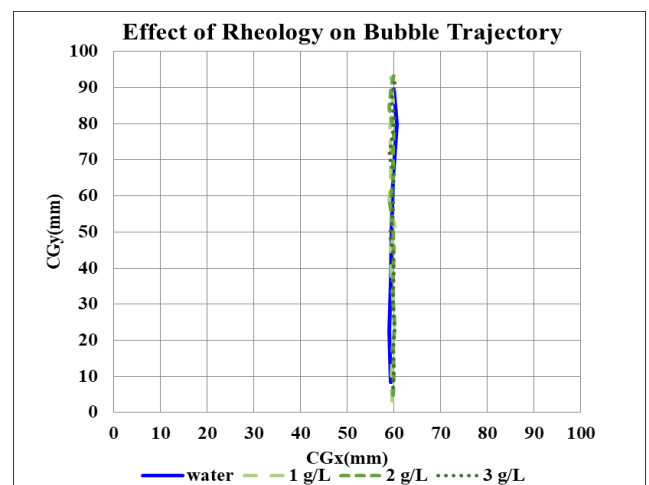


Fig. 10. Effect Of Rheology On Bubble Trajectory

4. Conclusion

The main aim of the current study was to investigate how fluid rheology, particularly viscosity changes, affects key hydrodynamic parameters like bubble size, terminal velocity, Reynolds number, bubble count, and trajectory. To measure and analyze bubble behavior using the shadowgraphy technique, providing quantitative insights into fluid-bubble interactions and providing actionable knowledge for optimizing gas-liquid interaction processes in CPIs by understanding the effects of rheology on bubble behavior. The study investigates the behavior of

bubbles in four fluids (water and CMC solutions with concentrations of 1 g/L, 2 g/L, and 3 g/L) by examining bubble diameter, terminal velocity, trajectory, Reynolds number, and bubble count. The key findings suggest that in water and CMC 1 g/L, bubble diameters are 1.48 mm. For higher-viscosity fluids (CMC 2 g/L and 3 g/L), bubble sizes increase to 1.86 mm and 2.08 mm, respectively, due to slower bubble detachment. The terminal Velocity for Water (Newtonian fluid) exhibits the highest terminal velocity (0.226 m/s). CMC solutions show progressively lower terminal velocities with increasing viscosity, ranging from 0.115 m/s (1 g/L) to 0.088 m/s (3 g/L). The bubble rising in Water has the highest Reynolds number (335.273), indicating a relatively turbulent flow. CMC solutions have significantly lower Reynolds numbers (31.522, 7.893, and 3.591 for 1 g/L, 2 g/L, and 3 g/L, respectively), suggesting laminar flow. It was found that in a water environment, fewer bubbles (7 per frame) compared to CMC solutions (14, 15, and 17 bubbles per frame for 1 g/L, 2 g/L, and 3 g/L, respectively) were produced. Finally, the trajectories in water and CMC solutions suggested that Bubbles in water follow a zigzag trajectory, while in CMC solutions, they follow rectilinear paths due to higher viscosity. The findings enable better design and operation of bubble column reactors by tailoring process parameters to the rheological properties of the liquid phase. Improved understanding of bubble dynamics in non-Newtonian fluids can enhance mass transfer efficiency and mixing in CPIs, leading to higher process yields. The study suggests that future work could include using different liquid phases (e.g., glycerol), examining bubble swarm behavior, studying rheological properties, and employing varying column thicknesses or capillaries.

5. References

- [1] A. Esmaili, C. Guy, and J. Chaouki, "The effects of liquid phase rheology on the hydrodynamics of a gas-liquid bubble column reactor", *Chem. Eng. Sci.*, vol. 129, pp. 193–207, 2015.
- [2] S. Almani, W. Blel, E. Gadoin, and C. Gentric, "Investigation of single bubbles rising in Newtonian and non-Newtonian fluids inside a thin-gap bubble column intended for microalgae cultivation", *Chem. Eng. Res. Des.*, vol. 167, pp. 218–230, Mar. 2021.
- [3] S. Almani, W. Blel, E. Gadoin, and C. Gentric, "Global characterization of hydrodynamics and gas-liquid mass transfer in a thin-gap bubble column in presence of Newtonian or non-Newtonian liquid phase", *Chem. Eng. Sci.*, vol. 282, no. September, p. 119291, 2023.
- [4] C. Thobie, E. Gadoin, W. Blel, J. Pruvost, and C. Gentric, "Global characterization of hydrodynamics and gas-liquid mass transfer in a thin-gap bubble column intended for microalgae cultivation", *Chem. Eng. Process. Process Intensif.*, vol. 122, pp. 76–89, 2017.
- [5] M. Asim et al., "Isolated bubble ascent in a non-Newtonian media inside an infinite bubble column: a CFD study", *Brazilian J. Chem. Eng.*, no. 0123456789, 2023.
- [6] A. Haydar, W. Blel, H. Marec, and C. Gentric, "Gas Holdup and Flow Regimes in a Thin-Gap Bubble Column with Newtonian and Non-Newtonian Liquid Phase", *Chem. Eng. Technol.*, vol. 46, no. 6, pp. 1218–1227, 2023.
- [7] K. Loubière and G. Hébrard, "Influence of liquid surface tension (surfactants) on bubble formation at rigid and flexible orifices", *Chem. Eng. Process. Process Intensif.*, vol. 43, no. 11, pp. 1361–1369, 2004.
- [8] G. Besagni and F. Inzoli, "The effect of liquid phase properties on bubble column fluid dynamics : Gas holdup , flow regime transition , bubble size distributions and shapes , interfacial areas and foaming phenomena", *Chem. Eng. Sci.*, vol. 170, pp. 270–296, 2017.
- [9] P. Pan, S. J. Li, H. L. Wei, X. B. Zhang, and Z. H. Luo, "Bubble columns with internals: A review on research methodology and process intensification", *Chem. Eng. Process. - Process Intensif.*, vol. 209, no. November 2024, p. 110156, 2025.
- [10] P. Luty, M. Prończuk, and K. Bizon, "Experimental verification of different approaches for the determination of gas bubble equivalent diameter from optical imaging", *Chem. Eng. Res. Des.*, vol. 185, pp. 210–222, 2022.
- [11] S. Liu et al., "Effects of internals on macroscopic fluid dynamics in a bubble column", *Chinese J. Chem. Eng.*, vol. 77, pp. 19–29, 2025.
- [12] V. V. Ranade, S. Marchini, R. Kipping, N. V. Ranade, and M. Schubert, "Estimation of gas hold-up in bubble columns using wall pressure fluctuations and machine learning", *Chem. Eng. J.*, vol. 500, no. October, p. 157078, 2024.
- [13] Z. Yao et al., "Effects of gas distributor on hydrodynamics in gas-liquid bubble column by

- visual experiments and CFD simulations”, *Chem. Eng. J.*, vol. 504, no. September 2024, p. 158476, 2025.
- [14] M. W. Abdulrahman, “Modeling gas holdup in a multiphase oxygen slurry bubble column reactor for Cu-Cl hydrogen production using CFD”, *Results Eng.*, vol. 24, no. September, p. 102955, 2024.
- [15] H. Khan, P. Kováts, K. Zähringer, and R. Rzehak, “Experimental and numerical investigation of a counter-current flow bubble column”, *Chem. Eng. Sci.*, vol. 285, no. October 2023, 2024.
- [16] I. A. Evdokimenko et al., “Experimental and numerical study of wall phenomena of confined bubble flow in a square channel”, *Chem. Eng. Sci.*, vol. 301, no. September 2024, 2025.
- [17] D. D. McClure, N. Aboudha, J. M. Kavanagh, D. F. Fletcher, and G. W. Barton, “Mixing in bubble column reactors: Experimental study and CFD modeling”, *Chem. Eng. J.*, vol. 264, pp. 291–301, 2015.
- [18] M. Zedníková, S. Orvalho, M. Fialová, and M. C. Ruzicka, “Measurement of volumetric mass transfer coefficient in bubble columns”, *ChemEngineering*, vol. 2, no. 2, pp. 1–14, 2018.
- [19] N. Garci and F. Garci, “Mixing in bubble column and airlift reactors”, vol. 82, no. October, pp. 1367–1374, 2004.
- [20] C. Thobie, E. Gadoin, W. Blel, J. Pruvost, and C. Gentric, “Chemical Engineering & Processing: Process Intensification Global characterization of hydrodynamics and gas-liquid mass transfer in a thin-gap bubble column intended for microalgae cultivation.”, *Chem. Eng. Process. Process Intensif.*, vol. 122, no. July, pp. 76–89, 2017.
- [21] W.D Deckwer, *Bubble Column Reactors*. Wiley. New York, 1991.
- [22] N. Kantarci, F. Borak, and K. O. Ulgen, “Bubble column reactors”, *Process Biochem.*, vol. 40, no. 7, pp. 2263–2283, 2005.
- [23] R. Krishna and J. M. van Baten, “Scaling up bubble column reactor with the aid of cfd”, *ICHEME*, vol. 79, Part A, no. April, pp. 283–309, 2001.
- [24] M. Berovič, T. Koloini, E. S. Olsvik, and B. Kristiansen, “Rheological and morphological properties of submerged citric acid fermentation broth in stirred-tank and bubble column reactors”, *Chem. Eng. J. Biochem. Eng. J.*, vol. 53, no. 2, 1993.
- [25] L. Böhm and M. Kraume, “Fluid dynamics of bubble swarms rising in Newtonian and non-Newtonian liquids in flat sheet membrane systems”, *J. Memb. Sci.*, vol. 475, pp. 533–544, 2015.
- [26] A. Souliès, J. Pruvost, J. Legrand, C. Castelain, and T. I. Burghelea, “Rheological properties of suspensions of the green microalga *Chlorella vulgaris* at various volume fractions”, *Rheol. Acta*, vol. 52, no. 6, pp. 589–605, Jun. 2013.
- [27] A. Souliès, J. Pruvost, J. Legrand, C. Castelain, and T. I. Burghelea, “Rheological properties of suspensions of the green microalga *Chlorella vulgaris* at various volume fractions”, *Rheol. Acta*, pp. 1–6, 2013.
- [28] J. Pruvost, F. Le Borgne, A. Artu, and J. Legrand, “Development of a thin-film solar photobioreactor with high biomass volumetric productivity (AlgoFilm©) based on process intensification principles”, *Algal Res.*, vol. 21, pp. 120–137, 2017.
- [29] M. van Sint Annaland, N. G. Deen, and J. A. M. Kuipers, “Numerical simulation of gas bubbles behaviour using a three-dimensional volume of fluid method”, *Chem. Eng. Sci.*, vol. 60, no. 11, pp. 2999–3011, Jun. 2005.
- [30] T. A. Pimenta and J. B. L. M. Campos, “Heat transfer coefficients from Newtonian and non-Newtonian fluids flowing in laminar regime in a helical coil”, *Int. J. Heat Mass Transf.*, vol. 58, no. 1–2, pp. 676–690, 2013.
- [31] R. Clift, J. R. Grace, and M. E. Weber, *Bubbles, drops and particles*. NY: Academic Press, 1978.
- [32] K. Dewsbury, D. Karamanev, and A. Margaritis, “Hydrodynamic characteristics of free rise of light solid particles and gas bubbles in non-Newtonian liquids”, *Chem. Eng. Sci.*, vol. 54, no. 21, pp. 4825–4830, Nov. 1999.
- [33] Z. Yujie, L. Mingyan, X. Yonggui, and T. Can, “Three-dimensional volume of fluid simulations on bubble formation and dynamics in bubble columns”, *Chem. Eng. Sci.*, vol. 73, pp. 55–78, 2012.
- [34] S. Almani, W. Blel, E. Gadoin, and C. Gentric, “CFD simulation of isolated bubbles rising in Newtonian or non-Newtonian fluids inside a thin-gap bubble column”, *Chem. Eng. Res. Des.*, vol. 214, no. December 2024, pp. 202–218, 2025.